ELSEVIER

Chemical Physics 239 (1998) 511–524

Chemical Physics

Anion spectroscopy of uracil, thymine and the amino-oxo and amino-hydroxy tautomers of cytosine and their water clusters

J. Schiedt [a], R. Weinkauf [a,*], D.M. Neumark [b], E.W. Schlag [a]

[a] *Institut für Physikalische und Theoretische Chemie der Technischen Universität München, Lichtenbergstrasse 4, 85747 Garching, Germany*
[b] *Department of Chemistry, University of California, Berkeley, CA 94720, USA*

Received 15 August 1998

Abstract

In this work we investigate different forms of electron binding in the mass-selected and cooled nucleobases uracil, thymine and cytosine and their water clusters. In photodetachment–photoelectron spectra of the pyrimidine nucleobases, sharp structures were found at 86 ± 8 meV (uracil), 62 ± 8 meV (thymine) and 85 ± 8 meV (cytosine), which are due to photodetachment of dipole-bound states. The photodetachment angle dependence of these states shows mostly p-wave detachment, which confirms the predicted predominant s-character of the electronic wave function of dipole-bound states. This anisotropy of electron emission and their sharp photodetachment structures can be taken for dipole-bound state recognition. Water attachment to the nucleobases results in positive valence-bound electron affinity, s-wave detachment and broad spectra, implying that the electron now is trapped inside the π^* LUMO of the nucleobases, stabilized by the water dipole. The solvent shifts in dependence on water aggregation are linear and allow by extrapolation an estimation of the monomer electron affinities. All three pyrimidine nucleobases are estimated to have a very similar valence-bound electron affinity in the range of 0–200 meV. In nucleobase $\cdot$ $(H_2O)_n$ clusters, due to the large total dipole moment, dipole-bound states also exist. Resonant excitation of these dipole-bound states with a photon of 1064 nm wavelength causes dissociation of the anion cluster, leading to monomer anions in their dipole-bound state. These monomer anions can be photodetached by a second IR photon. Whereas, for uracil and thymine, one dipole-bound state is detected, for cytosine we find two dipole-bound states (85 ± 8, 230 ± 8 meV) which are attributed to the dipole-bound states of the simultaneously present amino-hydroxy and amino-oxo cytosine tautomers. We also give a possible explanation why the formation of the dipole-bound state of the amino-oxo tautomer at 230 meV is improbable in the supersonic expansion.

1. Introduction

Charge transfer (CT) in deoxyribonucleic acid (DNA) is a subject of recent scientific interest [1–5] and is discussed with much controversy [6–8]. In DNA a surplus charge causes reactivity as shown by the examples of the electron-induced thymine dimer repair mechanism [2,9] and the positive charge-induced damage of guanine–guanine sequences [5,10]. Hence, the ability of DNA to move charges, and especially electrons along the π stack of the nucleobases, is of fundamental interest. This is especially so because charge-induced damage of certain DNA sequences or charge-induced repair of other DNA

---

[*] Corresponding author.

PII: S0301-0104(98)00361-9

sequences could be important mechanisms in respect to gene stability.

Charge transfer through DNA is typically investigated by attaching or intercalating donor and acceptor chromophores (typically large π systems). In the superexchange CT theory, donor and acceptor are electronically coupled via the bridge orbitals [11]. This coupling depends on the energetic matching between the donor and acceptor π^* orbitals to the bridge π^* orbitals [12,13], which are consequently very close in energy. Calculated energy gap values cover the range of 2 eV [13] to 0.2 eV [14]. The latter value even results in a situation in which electron injection into the DNA becomes possible and charge transfer was even proposed to be possibly a hopping mechanism [14]. Therefore, the position of the π^* orbitals of the nucleic acid bases, as well as any new information about the property of nucleobases to stabilize a surplus electron in any state of aggregation such as in gas phase, in clusters, in solution or in DNA, is important. By the empirical 'Koopmans theorem' for anions [15] positions of π^* LUMO orbitals can be determined from valence-bound electron affinities (EA_{VAL}). Solvent shifts are important to extrapolate the monomer EA_{VAL} and to investigate solvent shell formation and other effects. For such investigations mass-selected and cooled isolated nucleobase anions and nucleobase cluster anions are very suitable.

The capability to stabilize a surplus electron in the nucleobases has been investigated for uracil, thymine and adenine by Rydberg electron transfer [16] and for uracil and thymine by photodetachment–photoelectron spectroscopy (PD-PES) [17]. It was found that isolated nucleobases can stabilize the surplus electron in a dipole-bound state. In these states the electron is bound to the rotating dipole moment mostly outside of the molecule, a situation similar to that for Rydberg states. As shown for uracil, even attachment of a single Ar atom stabilizes the surplus electron inside the π^* LUMO, i.e. the binding character changes from dipole-bound to valence-bound [18]. Although for the uracil monomer a positive valence-bound electron affinity EA_{VAL} of 30–60 meV was found, it is difficult to form such anions due to the large geometry shift between the neutrals and the anions [18]. A similar co-existence of both states has been found for the uracil–Xe cluster [19]. Such a switch from dipole- to valence-bound was also predicted by theory for attachment of water molecules to uracil [20,21].

An overview of the historical development of dipole-bound states as well as a detailed review are given in Refs. [22,23]. The first experimental observation and interpretation of dipole-bound anions was reported by Compton [24] and followed by Brauman [25], Haberland [26] and Lineberger [27,28]. The first PD-PES of dipole-bound anions was reported by Bowen [22]. A sophisticated investigation and production of dipole-bound states was performed by Rydberg electron transfer [23]. A lower threshold for the dipole moment ($\mu \sim 2$ Debye), necessary for the existence of a dipole-bound state, was calculated [29] and demonstrated [30,31]. The existence of even two dipole-bound states in very polar molecules is predicted [23,30,31] but, up to now, not found experimentally.

In this work we present PD-PE spectra of dipole-bound states of mass-selected uracil, thymine,

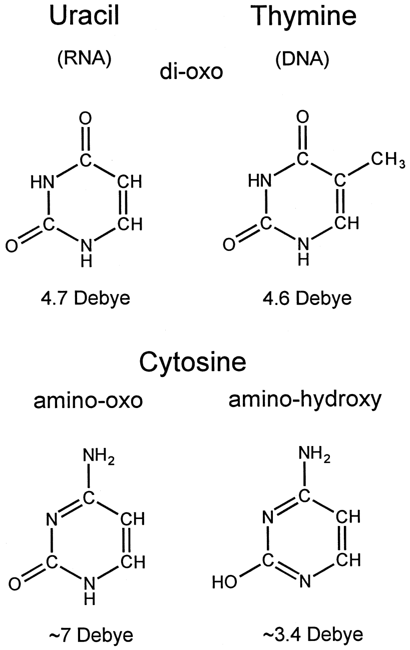

Fig. 1. Structure of the pyrimidine nucleic acid bases. Thymine (DNA) and uracil (RNA), which differ only by one methyl group, have at room temperature only a single tautomer. For cytosine the co-existence of two different tautomers with very different dipole moments has been found. The amino-oxo tautomer is the most stable tautomer ($\mu = 6.5$–8 Debye).

amino-oxo and amino-hydroxy cytosine (for structures see Fig. 1). Also the angle dependence of photodetachment from these dipole-bound states was measured. The PD-PE spectra of the pyrimidine nucleobase · $(H_2O)_n$ ($n = 1$–5) clusters are reported. Water shifts allow rough estimation of the valence-bound electron affinities and π^* LUMO positions of the nucleobase monomers. By IR excitation we find dissociation in dipole-bound states of the water clusters, which results in dipole-bound monomer anions. We even observe the presence of two tautomers for cytosine with this technique.

2. Experimental setup

The detailed experimental setup is described elsewhere [32]. It consists of an anion source, an ion extraction and acceleration zone, a quadrupole mass selector and a time-of-flight (TOF) photoelectron spectrometer. The anions and anion water clusters of the nucleobase were formed in a supersonic N_2 expansion (8 bar N_2 back-pressure mixed with traces of water and sample molecules) close to the pulsed and heated nozzle (50 Hz repetition rate) by attachment of low-energy electrons. These electrons were produced as secondary electrons by ionization of carrier gas molecules with primary high-energy electrons (1 keV). The latter are generated in a microchannel plate electron gun [32]. In order to achieve suitable sample vapour pressure of uracil, thymine and cytosine the nozzle was heated up to 200–250°C. After passing the heated skimmer, the anions were extracted perpendicular to the neutral jet by applying a pulsed voltage to deflection plates and then focussed into a quadrupole mass filter. The mass-selected anions were accelerated to about 200 eV kinetic energy and introduced into a TOF photoelectron spectrometer ($L = 468$ mm). Photodetachment is performed by the fundamental or second harmonic of a Nd:YAG laser (pulse width: 12 ns; pulse energy: 30 mJ at 1064 nm and 20 mJ at 532 nm). By calibration with atomic oxygen anions an electron energy resolution of 3 meV for photoelectrons of a kinetic energy of about 40 meV could be achieved. The experimental shift in absolute electron energy was estimated to be below 5 meV at such low excess energies. For high-energy electrons, the energy resolution and the accuracy in peak position is limited by the laser pulse duration of about 12 ns.

3. Results and discussion

In Section 3 we present (1) PD-PE spectra of dipole-bound states of the nucleobases uracil, thymine and amino-hydroxy cytosine, (2) the photodetachment anisotropy produced by dipole-bound states, and (3) photodetachment spectra of nucleobase · $(H_2O)_n$ clusters. We show that (4) in nucleobase · $(H_2O)_n$ clusters resonant photoexcitation of dipole-bound states is possible. In the subsequent dissociation of these states the surplus electron functions as a spectator. Finally (5) we interpret the presence of two dipole-bound states for the monomer fragment anions of cytosine as evidence for the presence of two conformers.

3.1. Dipole-bound anion states

The PD-PE spectra of the nucleobases uracil (a), thymine (b) and cytosine (c) measured at a detachment wavelength of 1064 nm (horizontal polarization) are presented in Fig. 2. Each spectrum shows one prominent, sharp peak at low binding energy (the anion ground-state energy is the origin of the energy scale). The sharp spectra of uracil and thymine agree well with previous spectra measured by Bowen and co-workers [17]. Based on the Franck–Condon principle a single prominent sharp peak indicates similar geometries between anion and neutral structure. Such behavior is expected of dipole-bound anion states where the surplus electron is mostly outside of the molecule as a spectator, i.e. the core is mostly neutral and not influenced by the charge. Therefore, for uracil and thymine, the sharp peaks in PD-PE [17] and Rydberg electron transfer spectra [16,18] have been attributed to the (0–0)-transition from the dipole-bound anion ground state to the neutral ground state. Here we add cytosine as the third pyrimidine base.

From peak positions the binding energies of the dipole-bound states are determined to be 86 ± 8 meV for uracil, 62 ± 8 meV for thymine and 85 ± 8 meV for cytosine. Due to the high excess energy of the photoelectrons (> 1 eV), the experimental elec-

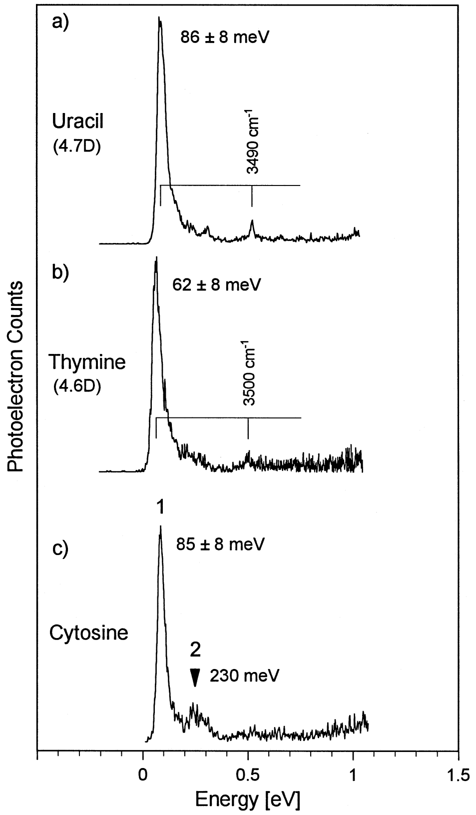

Fig. 2. Photodetachment–photoelectron spectra of the isolated nucleobase monomers uracil, thymine and cytosine. The predominant peaks are attributed to the 0–0 origin transitions from the dipole-bound anion to the neutral ground state.

tron energy resolution is limited by the laser pulse duration resulting in a peak width of about 40 meV and a peak position accuracy of about ±8 meV. Our values for uracil and thymine agree well with the results of Bowen and co-workers (PD-PES: uracil, 93 ± 7 meV; thymine, 69 ± 7 meV [17]), Schermann and co-workers (Rydberg electron attachment: uracil, 85 ± 15 meV [18]; thymine, 68 ± 20 meV [16]) and ab initio calculation of Adamowicz and co-workers (uracil, 86 meV [33]; thymine, 88 meV [34]). The dipole moments of uracil (4.7 Debye) [35] and thymine (4.6 Debye) [35,36] agree reasonably well with the binding energies expected for such dipole moments [23].

For cytosine, however, the observed binding energy of 85 ± 8 meV is surprising low considering that the cytosine dipole moment is predicted to be in the range of 6.5–8 Debye. The expected electron binding energy to a molecule of a dipole moment of 7 Debye is about 175 meV [23]. The binding energy of 85 ± 8 meV is expected to correspond to a dipole moment of 4–5 Debye. Looking for an explanation, we find that two cytosine tautomers have similar ground-state energies and can co-exist at room temperature in gas phase [37]. Although the amino-oxo tautomer presumably is somewhat more stable than the amino-hydroxy tautomer (see Table 2) at a nozzle temperature of 200–250°C, we expect both tautomers to have a comparable population. The tautomers have very different dipole moments of about 7 Debye for amino-oxo cytosine and 3.4 Debye for amino-hydroxy cytosine (Tables 1 and 2). To match binding energy and dipole moment, we attribute the sharp prominent peak in the PD-PE spectrum in Fig. 2c to the amino-hydroxy tautomer. Consequently we then assign the small broader peak at about 230 meV to the dipole-bound state of the amino-oxo tautomer. This assignment brings the expected large dipole moment of 7–8 Debye for amino-oxo cytosine into qualitative agreement with the electron binding energy of 230 meV. The intensity difference between the two peaks is, however, remarkable. Although theory predicts [37] and experiments show [43] that both tautomers have similar energy and should have similar population, their peak intensities are very different, i.e. the population in the amino-oxo tautomer anion is very small. This lack of amino-oxo tautomer intensity in the PD-PE spectrum is explained in Section 3.5. The exact energy of the dipole-bound state of the amino-oxo tautomer is determined by a two-photon excitation involving anion cluster dissociation as described in Section 3.4.

Table 1
Dipole moments μ, dipole-bound electron affinity EA_{DB} and relative stability ΔE and of the two most stable tautomers for uracil

	Reference	Di-oxo	Oxo-hydroxy
μ (Debye)	calc. [37]	4.4–4.5	3.2–3.3
	calc. [38]	4.2–4.9	3.4–3.6
	calc. [35]	4.7	
	est./exp. [39]	3.9	
	est./exp. [40]	4.2	
EA_{DB} (meV)	this work	86 ± 8	–
ΔE (meV)	calc. [37]	0	~ 470–490

Table 2
Dipole moments μ, dipole-bound electron affinities EA_{DB} and relative stability ΔE of the two most stable tautomers for cytosine. Note the large dipole moment for amino-oxo cytosine

	Reference	Amino-oxo	Amino-hydroxy
μ (Debye)	calc. [37]	6.5–6.7	3.4–3.5
	calc. [41]	7.12	3.4
	calc. [36]	7.16	
	est./exp. [41]	6.5	
	est./exp. [40]	7.65	
	est./exp. [42]	8.0	
EA_{DB} (meV)	this work	230 ± 8	85 ± 8
ΔE (meV)	calc. [37]	0	~ 16–43
	exp. [43]	0	~ 0

For uracil and thymine, the other possible tautomers (oxo-hydroxy, di-hydroxy and others) are much higher in energy than the most stable di-oxo tautomer [37]. They are, therefore, not populated even at the high temperatures (200–250°C) we used for evaporation. The weak structures in the PD-PE spectra (Fig. 2a,b) at higher energies are attributed to transitions to vibrational excited neutral states [17], which have small intensities because of the similar geometry between the dipole-bound anion and the neutral structure.

3.2. Angle-resolved photodetachment of dipole-bound states

Due to the special binding situation in dipole-bound anions, an investigation of the angle dependence of the PD process was considered to be very interesting to identify the electronic wave function involved. Fig. 3 shows, for uracil, the dependence of the total photoelectron signal on the polarization angle of the detachment laser (wavelength: 1064 nm). The data are fitted with the function $d\sigma/d\Omega \sim [1 + \beta \cdot P_2(\cos\theta)]$ (solid line) with an anisotropy parameter of $\beta \approx 1.4$. The signal is composed of a large $(\cos\theta)^2$ contribution corresponding to a p-wave photodetachment ($\beta = 2$) and an angle-independent contribution which is attributed to s-wave detachment ($\beta = 0$) [44]. The angle-resolved detachment spectra for thymine and cytosine show the same behavior (not shown here).

The angular momentum of the emitted electron (p-wave photodetachment: $l = 1$) is expected to depend via angular momentum conservation on the angular momentum of the initial anion state, the final neutral state (here $l = 0$) and the photon ($s = 1$) [44]. Hence, the p-wave detachment containing some contribution of s-wave detachment ($\beta = 0$) reveals the character of the electronic wave function as an s-orbital with some p-orbital contribution. This nicely confirms model calculations which predict that dipole-bound states have an electronic wave function of s-character with some minor p_z-orbital contribution [23]. Such dipole-bound state electronic wave functions of spherical shape, strongly displaced from the molecular centre, are given in many references [21,23,33,34,45–49]. The p-wave detachment of dipole-bound states found here gives us a new criterion for identifying such states (see Section 3.4). Distinctly different laser polarization dependence was also found for co-existing dipole- and valence-bound states in pyridine tetramer anions [50].

The pyrimidine nucleobases can stabilize a surplus electron in dipole-bound states. They are a property of the isolated molecules in the gas phase and have little direct relevance for processes or properties of the nucleobases in solvents or within DNA and RNA structures. Therefore in a second step it is highly interesting also to study the properties of nucleobases in its native environment such as in water.

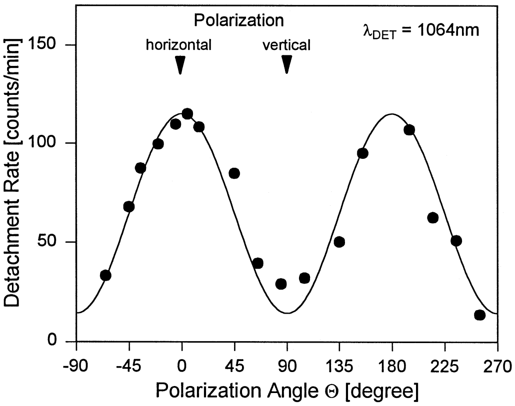

Fig. 3. Dependence of the photodetachment signal of the dipole-bound states on the polarisation angle of the detachment laser. The $\cos^2(\theta)$ photoelectron emission behavior (solid line) corresponds to a p-wave photodetachment (anisotropy parameter $\beta = 1.4$). Beside the narrow shape the p-wave detachment is now an additional criterion for the identification of dipole-bound states.

3.3. Water clusters: valence-bound anion states

It is well known that EAs strongly depend on solvation [51–53]. For the nucleobases the question arises how the properties of electron stabilization change in aqueous environment. In mass-selected clusters we even can pose more specific questions such as how many water molecules are needed to obtain a positive EA_{VAL} and how does the EA_{VAL} shift with cluster size. Fig. 4 presents PD-PE spectra of the nucleobase $\cdot (H_2O)_n$ clusters ($n = 0$–5) of uracil (a), thymine (b) and cytosine (c). For all nucleobases the same behavior can be observed. Already the attachment of one water molecule causes a dramatic change in the energetic position as well as in the shape of the PD-PE spectra. Instead of the sharp prominent peak at low energy (see bottom of Fig. 4), a rather broad structure at significant higher energy is found. This has also been observed before for uracil $\cdot (H_2O)$ and uracil $\cdot$ Xe anion clusters [19] and is a typical indication for clusters distorted by the electron localized inside the cluster. Because one water molecule itself is not able to stabilize an electron, this implies that uracil–water, thymine–water and cytosine–water (both tautomers) form valence-bound anions with the surplus electron now residing in the π^* LUMO of the nucleobases [51,52,54,55]. Thus the spectra show that the nucleic acid bases in aqueous environment have positive EA_{VAL} as predicted by Sevilla et al. [56] and already shown for uracil by Bowen [19] and Schermann and co-workers [18].

An ab initio investigation for the uracil $\cdot (H_2O)_3$ cluster [20] gives a vertical EA_{VAL} of 0.9–1.1 eV which is somewhat below the peak maximum of our corresponding PD-PE spectrum (Fig. 4). However, a

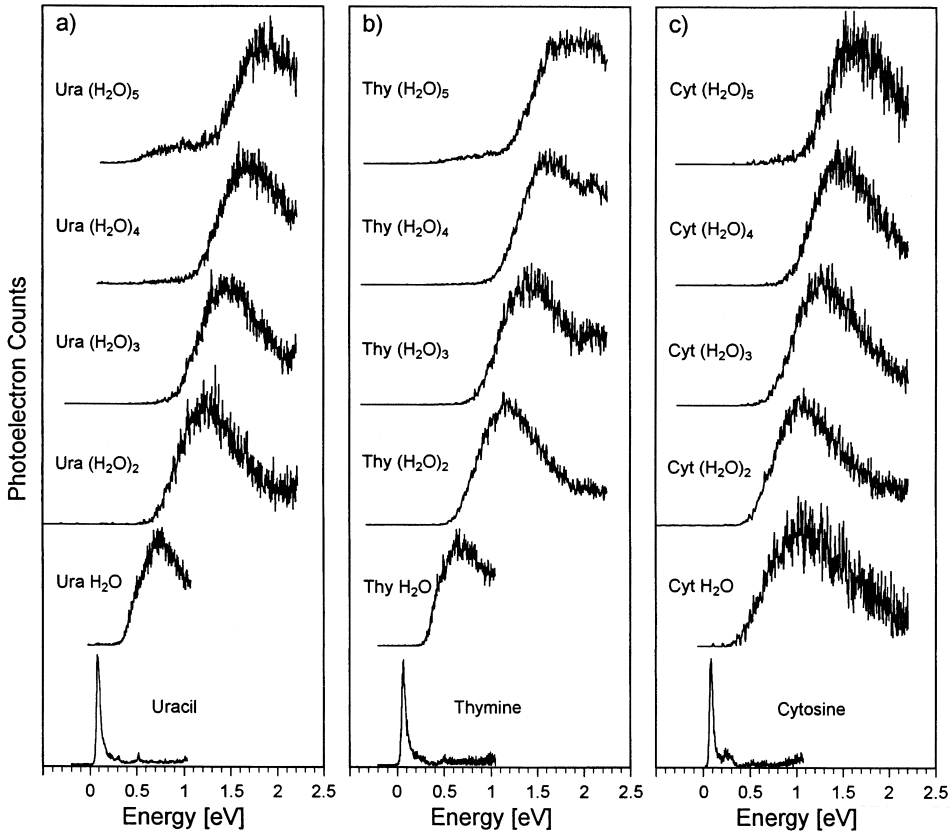

Fig. 4. PD-PE spectra of uracil (a), thymine (b) and cytosine (c) and their water clusters. The broad cluster spectra indirectly show that the electron is localized in the π^* LUMO of the pyrimidine nucleobases.

small negative adiabatic EA_{VAL} within the range between -0.07 and -0.24 eV was calculated, which does, however, not fit together with the existence of stable ($\tau > 250$ μs) valence-bound uracil $\cdot (H_2O)_3$ anions. Also Rydberg electron transfer experiments of Defrancois et al. clearly show that the anion state is below the neutral molecule [18]. Nevertheless, the calculations [20] confirm large differences in geometry between anion and neutral nucleobase $\cdot (H_2O)_n$ clusters. Thus, the determination of absolute adiabatic EA_{VAL} values by the onset of the structures in the PD-PE spectra should be done with caution. The determination of relative EA_{VAL} values, however, within one series of water clusters is reliable.

With increasing size of the water clusters, the onset of the structure in the PD-PE spectra shifts towards higher energies. The electron affinities determined from the onsets have an accuracy of about 100 meV. They are displayed in Fig. 5 in dependence on cluster size *n*. For all three bases no saturation in increase of EA_{VAL} can be observed. Furthermore the increase with cluster size seems to be linear within the accuracy of the measurement. The average increase per added water molecule is 0.22 eV for uracil, 0.20 eV for thymine and 0.17 eV for cytosine, i.e. rather small. A comparison with the solvation behavior of point charges (O_2^-: $\Delta E = 800$ meV [57]) and anions with an extended π systems (anthracene$^-$: $\Delta E = 240$ meV [54,58]) indicates that, in the pyrimidine nucleobases, the surplus charge is delocalized in the π system.

As for EAs and π^* positions, extrapolation of the slope to the origin (monomer base) would give positive but small values for EA_{VAL} of 150 ± 120 meV (uracil), 120 ± 120 meV (thymine) and 130 ± 120 meV (cytosine, both tautomers). These results show that EA_{VAL} is close to zero but, even more interesting, is very similar for the three pyrimidine bases studied. Due to the geometry shift between the anion and the neutral cluster and the inaccuracy in determination of the adiabatic EA_{VAL}, the error margins are large (± 120 meV). In this uncertainty we also included that this procedure might be slightly wrong because the EA_{VAL} could change somewhat more by adding the first water molecule than the second, i.e. the behavior of the EA_{VAL} should not be linear within this region (see Fig. 5). In Table 3 experimental and theoretical values for EA_{VAL} are compared. Employing 'Koopmans theorem' for anions [15], we can estimate the π^* LUMO to be situated at -2.0 ± 0.14 eV for all pyrimidine nucleobases. This narrow range for the π^* orbitals of the pyrimidine nucleobases provides an ideal resonance condition for the DNA bridge concerning electron transfer. The question still open is where the π^* LUMOs of the purine nucleobases are situated.

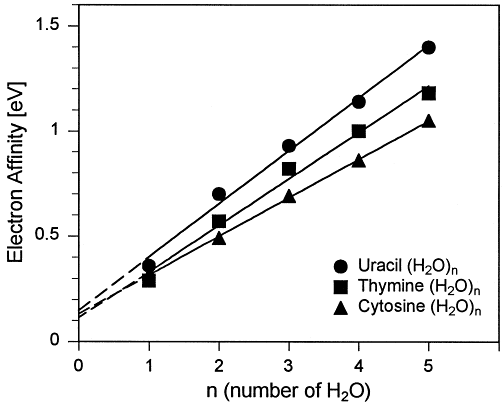

Fig. 5. Dependence of the electron affinity (onset) on the size *n* of the nucleobase $\cdot (H_2O)_n$ clusters. The shift increment decreases from uracil via thymine to cytosine and can be correlated with the size of the molecule and the size of the π system. The solvent shift extrapolation allows an estimation of the electron affinities for valence-bound anions of the pyrimidine nucleobases. Note that all electron affinities, and hence all π^* LUMO energies are very similar.

In situ, e.g. in DNA in a polar solvent environment, a lowering of the electron energy in the π^* LUMO can be assumed due to (i) stabilization by the polarizability of the π stack, (ii) the dipole moments of bound water and (iii) the hydrogen bond formation to the complementary base. The latter is a situation close to a solvation by two bound waters. The question how the water molecules are bound to the nucleobases is still open. For solvation of anions spectroscopy [61] and calculations [62] show that water tends to form one-sided sub-clusters in which each water molecule binds with one hydrogen to a neighbouring water forming ring systems ($n = 1$–5) and then three-dimensional structures ($n \geqslant 6$). This concept would also agree here with the observed linear shift of EA_{VAL} in dependence on cluster size. This would be, however, in contradiction to ab initio calculations of Adamowicz and co-workers [20] who

Table 3
Comparison of valence-bound electron affinities for the three pyrimidine nucleobases. The energy of the LUMO orbital E_{LUMO} is calculated by the formula $E_{\mathrm{LUMO}} = -\mathrm{EA}_{\mathrm{VAL}} - 1.9$ eV [15]

Uracil	Thymine	Cytosine (amino-oxo)	Remark	Ref.
150 ± 120 meV	120 ± 120 meV	130 ± 120 meV	water shift extrapolation	this work
30–60 meV	–	–	Rydberg electron transfer	[18]
−220 meV	−290 meV	−320 meV	electron attachment	[59]
−190 meV	−320 meV	−400 meV	calc.	[60]
20 meV	–	−240 meV	calc.	[15]
-2.05 ± 0.12 eV[a]	-2.02 ± 0.12 eV[a]	-2.03 ± 0.12 eV[a]	E_{LUMO}	this work

[a] E_{LUMO} calculated with values of line 1.

predicted that the first three water molecules are hydrogen bound to the uracil anion and form the first solvation shell.

3.4. Nucleobase · $(H_2O)_2$ clusters: resonant excitation of dipole-bound states with subsequent dissociation

Due to their large dipole moments also for the nucleobase · $(H_2O)_n$ clusters, the existence of dipole-bound states is expected [20,21,63]. As expected and found by the PD-PE spectra the cluster ground state is valence-bound. The dipole-bound state, hence, is the first excited cluster anion state. As shown by several groups [27,28,61,64] resonant transition from a valence-bound ground state to a dipole-bound excited state is possible. Due to the similarity of the geometry of dipole-bound anions and neutrals, vibrational states of the dipole-bound states are in the same way accessible as the corresponding neutral states. The questions we would like to address in the following are: do nucleobase · $(H_2O)_n$ clusters have dipole-bound states and are they observable, can we excite them, and what happens after their photoexcitation?

Fig. 6 shows PD-PE spectra of uracil · $(H_2O)_2$ and cytosine · $(H_2O)_2$ measured at wavelengths of 532 nm (a,c) and 1064 nm (b,d). In the 532 nm spectra the broad PD-PES structure of the valence-bound anion clusters of Fig. 4 are repeated. In the spectra recorded with a wavelength of 1064 nm (Fig. 6b,d) beside the broad structure one (uracil) respectively two (cytosine) additional sharp peaks appear at low energy. Similar spectra have been recorded also for thymine (not shown here). Also in thymine as in uracil they show for 1064 nm excitation one narrow peak at low energy.

The simplest explanation for the observation of the sharp peaks in the PD-PE spectra of the clusters at 1064 nm would be that, in the anion beam of the mass-selected clusters, beside the valence-bound also dipole-bound anion clusters are present. The observed structures at a detachment wavelength of 1064 nm would then be a superposition of PD-PE spectra arising from different types of anions. Such a situation was found by Bowen and co-workers for uracil · Xe cluster anions [19] and by Kim and co-workers for pyridine tetramer anions [50]. In this case, both types, i.e. dipole- and valence-bound anions, can co-exist because they are mostly isoenergetic and separated by a barrier. This spectra superposition of two anion species is expected to be independent on the detachment wavelength.

Because the sharp peaks in our spectra are not present at an excitation wavelength of 532 nm (at each laser polarization angle), the initial presence of two types of anions can be ruled out. Nevertheless the concept that the PD-PE spectra are due to two different types of anion species is convincing. We attribute the sharp peaks of Fig. 6b,d to a photodetachment of the dipole-bound nucleobase monomers, which are formed by resonant excitation from the valence-bound to a dipole-bound state of the cluster anion and its subsequent dissociation. The following properties of the sharp structures support this assignment:

(i) Their energetic position is the same for the nucleobase · $(H_2O)_n$ cluster of sizes $n = 2$ and $n = 4$ ($n = 4$ is not shown here) and, hence, they are not a property of the cluster size.

(ii) They are sharp and show the anisotropy behav-

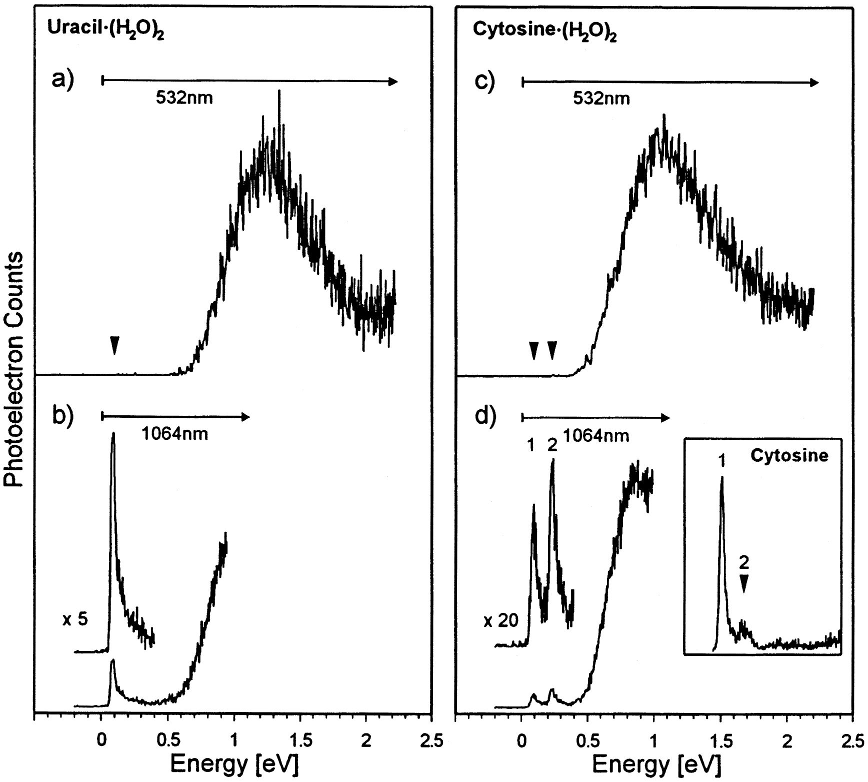

Fig. 6. PD-PE spectra of uracil · $(H_2O)_2$ (left) and cytosine · $(H_2O)_2$ (right) recorded with detachment wavelengths of 532 nm (a,c) and 1064 nm (b,d). In (b) beside the normal photodetachment photoelectron signal, for uracil and thymine (not shown) an additional sharp peak appears exactly at the energy of the dipole-bound anion state of the nucleobase monomer. In the case of cytosine (d) two additional peaks occur which are attributed to photodetachment of the dipole-bound states of the amino-hydroxy (85 meV) and the amino-oxo (230 meV) cytosine tautomers (see also text).

ior of dipole-bound states (p-wave detachment; see Fig. 3).

(iii) Their energetic position is the same as observed for the dipole-bound states of the isolated nucleobases (Fig. 2).

(iv) They appear only at 1064 nm but not at 532 nm anion cluster photoexcitation (see Fig. 6) which indicates that a resonant anion state is involved.

(v) They occur only for cluster size $n = 2$ and $n = 4$, which is an indication that the process might depend on the total cluster dipole moment.

In the following we propose a scenario which explains the experimental results (i)–(v). In Fig. 7a–c the energy scheme of a nucleobase · $(H_2O)_2$ cluster and the concerning monomer is presented. The proposed mechanism consists of (b) resonant photoexcitation ($h\nu_1$) into a dipole-bound state (dotted lines) of the cluster, (b_2) dissociation into the dipole-bound nucleobase monomer and neutral water and (c) photodetachment of the monomer dipole-bound state by a second photon ($h\nu_2$). Also autodetachment can compete with dissociation (b_1).

In the usual photodetachment process the anion is excited into the continuum (Fig. 7a). Dipole-bound cluster states, however, give rise to a large optical excitation cross-section [61] which competes efficiently (b) with the continuum excitation (a). Because water clusters, with their low-frequency librations, offer an enormously high density of vibrational states, the presence of a resonant excitation is always guaranteed even at the accidental wavelength of 1064 nm. The large anion to neutral geometry change of the clusters shows that high vibrational states of the dipole-bound state are accessible with a large

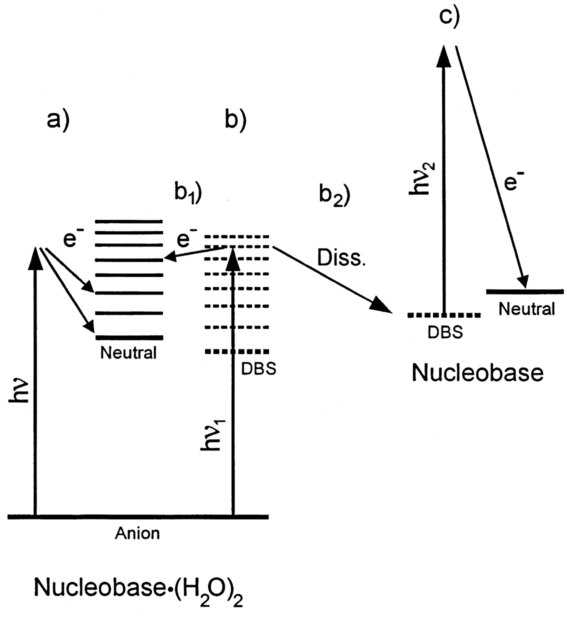

Fig. 7. Energy scheme of the nucleobase $\cdot(H_2O)_2$ cluster and the nucleobase monomer. Beside normal photodetachment into continuum (a) resonant excitation from the valence-bound anion ground state into high vibrations of the dipole-bound excited anion state (DBS) is possible (b). Beside vibrational autodetachment (b_1) dissociation of the anion cluster can take place (b_2). During this process the electron acts as a spectator. The dipole-bound state of the nucleobase monomer can be then photodetached by a second photon (c). This two-photon process only can take place if an excitation leads resonantly into the dipole-bound cluster state (see arrow length in Fig. 6). For cytosine the ratio of the two tautomers present in the heated nozzle is conserved in the water clusters and the fragment anion distribution, resulting in a dipole-bound state for each tautomer.

Franck–Condon factor. For the nucleobase $\cdot(H_2O)_2$ clusters, this is especially the case for an excitation in the range of 1064 nm (~ 1.2 eV). This photoexcitation leads in all nucleobase $\cdot(H_2O)_2$ anion clusters to a high vibrational energy of 0.5–0.7 eV in the dipole-bound state. The energy needed for the dissociation of the dipole-bound anion cluster is assumed to be very similar to the neutral cluster because of the electron being mostly outside of the cluster. The neutral binding energy for one water is estimated to be 0.2 eV, which corresponds to the breaking of a hydrogen bond to the nucleobase. Hence, after dipole-bound state excitation the internal cluster energy is large enough for complete loss of two water molecules (c). Although most of the excited dipole-bound state clusters may undergo vibrational autodetachment (b_1), for some clusters the electron obviously can act as a spectator of the core dissociation and survive in the dipole-bound state. During dissociation the dipole-bound state of the cluster is then converted into the dipole-bound state of the monomer. The monomer can be then photodetached by a second photon, explaining the sharp dipole-bound state structure in Fig. 6b,d. The low intensity of the monomer dipole-bound states in Fig. 6 is explained by the competition of the dissociation with (i) photodetachment into continuum, (ii) autodetachment from the highly excited dipole-bound states and (iii) radiationless recombination. This two-photon process involving cluster dissociation explains the exclusive observation of dipole-bound states at the IR wavelength, and all other experimental findings above. A direct two-photon process via a dipole-bound cluster state can be ruled out. Such a process would image the dipole-bound state of the cluster and its EA_{DB} should depend on cluster size. This, however, is in contrast to our finding that, for all pyrimidine nucleobases, the peak positions are constant for the anion cluster with two and four added water molecules. In addition, the energy exactly corresponds to the dipole-bound state of the respective isolated nucleobase.

In our experiment the fragmentation of the cluster dipole-bound state has to occur within the laser pulse in order to explain the fragment ion detachment. Such fast monomer anion formation out of a cluster has been found previously for O_4 [65], benzoquinone $\cdot H_2O$ [66] and azulene $\cdot H_2O$ [57] anion clusters. Ultrafast dynamics of dipole-bound states and anion fragmentation have also been observed in femtosecond experiments for $I\cdot(H_2O)^-_{5,6}$ clusters [67]. The finding that the dipole-bound electron acts like a spectator has analogy to Rydberg states where photofragmentation of the benzene core in the presence of a high quantum Rydberg state was also possible [68].

We tried to prove the two-photon character of the process by variations of the laser intensity but did not find significant effects. We explain this by saturation of the valence- to dipole-bound state transition, which typically has a large cross-section [61]. The dependence of the appearance of the dipole-bound monomer states on the number of water molecules (see v) is not yet understood completely. It seems to be coupled with a property of the cluster. Either the total dipole moment of some clusters is too small so that no dipole-bound state exists or the binding energy in the dipole-bound state is so small that autodetachment becomes very fast and anion fragmentation cannot compete. In tendency the latter explanation is confirmed by calculations for uracil, uracil · (H_2O) and uracil · $(H_2O)_3$ [20,21,33], showing that the cluster binding energies in the dipole-bound states are small. In any case, the appearance of dipole-bound monomer states only for nucleobase–water cluster sizes of two and four, but not one and three, water molecules clearly shows that the resonant excited anion cluster state is not of valence-bound character. If this were so, resonant excitation would take place between two valence-bound states (π^*–π^* or n–π^* [32]) of the nucleobases and, hence, would be independent on cluster size.

3.5. Distinction of two cytosine tautomers by PD-PES of dipole-bound anions

One interesting observation for cytosine (Fig. 6d) is the occurrence of two different dipole-bound states after cluster dissociation. For uracil and thymine, the monomer dipole-bound states formed via anion cluster dissociation correspond exactly in number and energy to the monomer dipole-bound state of the anions formed in the supersonic expansion. For cytosine the sharp peak 1 (Fig. 6d) is identified by energetic position with the spectrum of the monomer dipole-bound state (Fig. 2, see insert). Peak 2 at 230 meV is identified also to be a transition from a dipole-bound anion by its sharp structure and its p-wave detachment. For explanation of its nature we have two possibilities. It is (i) either a second dipole-bound state of one cytosine tautomer or (ii) a dipole-bound state of a second tautomer.

As for (i), for molecules of very large dipole moment the existence of two dipole-bound states was predicted [23,69]. Whereas the lower ground-state dipole-bound state is strongly bound, the excited state is supposed to have a very low binding energy below 10 meV [23]. Hence assignment of the two peaks to two dipole-bound states of one cytosine tautomer can be ruled out because of the large dipole-bound electron affinity EA_{DB} for both states.

As for the tautomer problem (ii), indeed we find in literature [37] for cytosine two tautomers of very similar stability but very different dipole moments of 6.5–8 and 3.4–3.5 Debye (see Table 1). With this information we attribute the two sharp peaks to the dipole-bound states of the amino-oxo (230 meV) and the amino-hydroxy cytosine tautomers (85 meV). The assignment for the structure at 230 meV (peak 2) to be a dipole-bound state of the amino-oxo cytosine tautomer is evident for the following reasons:

(i) Peak 2 shows the same dependence on detachment wavelength as peak 1: they vanish at 532 nm and appear at 1064 nm. This indicates that both are formed by the same mechanism.

(ii) It shows all characteristics of a dipole-bound state such as sharp peaks and p-wave detachment.

(iii) Due to the large binding energy, peak 2 should correspond to a large dipole moment of about 7 or more Debye [23] as expected for the amino-oxo tautomer (see Table 2).

(iii) The second peak only appears for cytosine, which has two tautomers of similar stability but very different dipole moments.

(iv) Peak 2 agrees in energy with the weak structure present in the PD-PE spectrum of the cytosine monomer.

Due to the similar stability [37] of the two cytosine tautomers, we can assume that, in our heated nozzle, both neutral tautomers are formed with a similar intensity. If this and the assignment of the dipole-bound states formed via the water cluster are correct, we have to explain why the dipole-bound state of the amino-oxo tautomer at 230 meV only has a very weak intensity in the PD-PE monomer spectrum (Fig. 2c). We believe that, in comparison to the amino-oxo, the amino-hydroxy tautomer anion is enhanced in the anion formation process taking place in our source. The reason for observation of the strongly bound dipole-bound state (I) via cluster fragmentation but not (II) in the direct anion formation process in the gas phase has to be found in the different nature of these monomer anion formation processes.

As for (I), in the cluster spectra (Fig. 6) the population of the dipole-bound monomer states results from a resonant excitation to the dipole-bound cluster state with a subsequent anion dissociation. Because both tautomers can be assumed to be present in the gas phase, both tautomers can be embedded into water clusters which then can attach electrons. These clusters can be photodissociated, resulting in two tautomers each in a dipole-bound anion state. Isomerization between the tautomers is assumed to be improbable because of the fast cooling in the expansion and the high barriers between tautomers.

As for (II), in the spectra of the monomer nucleobases (Fig. 2) the dipole-bound states are formed in the N_2 gas expansion, a completely different mechanism. We now raise the question which formation mechanisms of dipole-bound states take place in a supersonic expansion seeded with low and high energetic electrons. Several scenarios are possible:

(i) A free low energetic electron is captured into the dipole-bound state and the electron binding energy set free is transformed into vibrational energy. This process is very unlikely because the electron motion is fast (vertical process) and the dipole-bound anion and the neutral state have a very similar geometry (propensity rule $\Delta \nu = 0$).

(ii) The electron is captured without vibrational excitation and the binding energy is extracted in a three-body collision. Such a process is also improbable especially because the light electron is unable to efficiently transfer energy to heavy particles.

(iii) Electron attachment to clusters leading to dissociation into the monomer dipole-bound state. This process is similar to our proposed cluster photodissociation mechanism. For production of the dipole-bound monomer anion the dissociation from the dipole-bound cluster state is necessary (see i, ii, iv above). It is assumed, however, that the cluster anion formation leads predominantly to valence-bound clusters.

(iv) The electron is transferred from a mostly isoenergetic Rydberg state of the N_2 carrier gas into the dipole-bound state of the nucleobase. Those Rydberg states are supposed to be formed in the N_2 expansion mostly by primary electron collisions. This mechanism does not need further stabilization and results in cold dipole-bound anions.

We strongly favour route (iv) to be responsible for formation of dipole-bound anions in the supersonic expansion. Rydberg electron transfer has shown to be very efficient [23]. So how can we explain that the dipole-bound state of the amino-oxo cytosine tautomer at 230 meV binding energy is formed so weak? As shown by Desfrancois and Schermann [23] for efficient electron transfer a certain Rydberg level is the most efficient. The Rydberg quantum number n for maximum transfer rate can be estimated by $EA_{DB} = 23\ eV/n^{2.8}$. For $EA_{DB} = 230$ meV the Rydberg quantum number n is 5, i.e. rather low. For the two cytosine tautomers, the situation of dipole-bound anion formation is shown in Fig. 8. In (a) the amino-hydroxy and in (b) the amino-oxo tautomers of cytosine with their dipole-bound states at 85 and 230 meV below the threshold are shown. In (c) schematically a Rydberg state ladder is drawn. At 230 meV the Rydberg state density becomes very sparse. The efficiency of electron transfer from Rydberg orbitals being somewhat off-resonant decays exponentially with energetic distance from n_{max} [23]. Even the higher state density due to vibrations [70] in the molecule N_2 does not help because in molecules Rydberg states of low quantum numbers have short lifetimes. In addition, the size of the

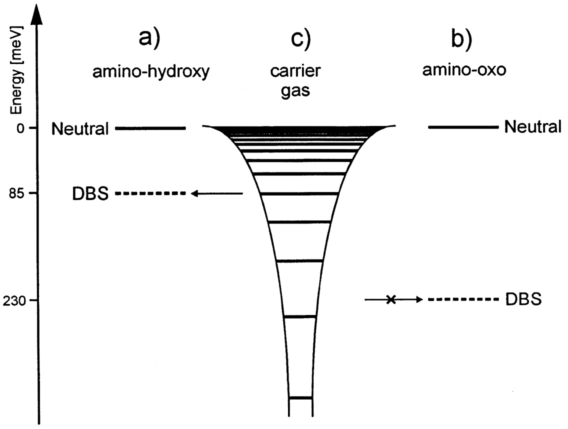

Fig. 8. Rydberg electron transfer scheme. (a) The amino-hydroxy tautomer and (b) the amino-oxo tautomer with their dipole-bound states at 85 and 230 meV. (c) The Rydberg state level scheme. At 230 meV below threshold (i) the Rydberg state levels are sparse, (ii) their lifetimes short and (iii) their orbital sizes small. All these arguments motivate that Rydberg electron transfer is not efficient for formation of dipole-bound states (DBS) of large binding energies.

electron orbitals becomes small for low n quantum numbers, thus reducing the interaction distance for electron transfer to a second molecule.

Hence, we have found good arguments that a dipole-bound state at 230 meV binding energy is formed with less efficiency by Rydberg electron transfer than a dipole-bound state at 85 meV. This could explain the small peak for the strongly bound dipole-bound state of the second tautomer, although the population of the corresponding neutral tautomer is sufficiently large. The result is that Rydberg electron transfer is obviously tautomer selective here.

4. Conclusion

In this work former results by Bowen and coworkers [17,19] concerning dipole-bound anion states of the nucleic acid bases uracil and thymine in gas phase could be confirmed. In addition, the energy of the dipole-bound state of two tautomers of the pyrimidine nucleobase cytosine was measured. Their electron affinities EA_{DB} are in agreement with the expected tautomer dipole moments. The anisotropy parameter for photodetachment of dipole-bound states was determined to $\beta \approx 1.4$ corresponding to mostly a p-wave detachment. This confirms the predicted predominant s-character of the electronic wave function of dipole-bound states.

All pyrimidine nucleobases have positive EA_{VAL} in aqueous environment and can incorporate the surplus electron into π^* LUMO, delocalized over the entire molecule. By water shift extrapolation it is found that the π^* LUMOs of all pyrimidine nucleobases are situated at low and very similar energies. This is an ideal precondition for an efficient nearest-neighbour coupling as necessary for charge transfer in DNA.

In the PD-PE spectra of nucleobase $\cdot (H_2O)_n$ anion clusters measured at IR wavelength a superposition of photodetachment from valence-bound as well as from dipole-bound anions is observed. This is explained by resonant excitation of high vibrations in the dipole-bound cluster excited state. The cluster then boils off the water molecules where the electron acts as a spectator. After dissociation of the anion cluster, the surplus electron stays in the dipole-bound state of the nucleobase monomers from which it can be photodetached by a second photon. By this complex monomer anion formation mechanism we find for cytosine in addition to the dipole-bound state at 85 meV a very strongly bound dipole-bound state at 230 meV. The latter is attributed to the dipole-bound state of the most stable amino-oxo cytosine tautomer, which has a very large dipole moment of 6.5–8 Debye. This tautomer anion was only very weakly observed by direct anion formation in the supersonic expansion. We tentatively explain this by an energy dependence of the efficiency of the Rydberg electron transfer from the excited carrier gas molecules to the nucleobases.

Acknowledgements

We thank J.-P. Schermann, C. Desfrançois and B. Brutschy for interesting discussions. We also gratefully acknowledge the support of the ‘Deutsche Forschungsgemeinschaft’. DMN thanks the ‘Alexander von Humboldt Stiftung’ for support.

References

[1] F.D. Lewis, T. Wu, Y. Zhang, R.L. Letzinger, S.R. Greenfield, M.R. Wasielewski, Science 277 (1997) 673.
[2] P.J. Dandliker, R.E. Holmlin, J.K. Barton, Science 275 (1997) 1465.
[3] E.D.A. Stemp, M.R. Arkin, J.K. Barton, J. Am. Chem. Soc. 119 (1997) 2921.
[4] G. Taubes, Science 275 (1997) 1420.
[5] D.B. Hall, R.E. Holmlin, J.K. Barton, Nature 382 (1996) 731.
[6] U. Diederichsen, Angew. Chem. 109 (1997) 2411.
[7] J.M. Warman, M.P. de Haas, M. Rupprecht, Chem. Phys. Lett. 249 (1996) 319.
[8] S. Poryadarshy, S.M. Risser, D.N. Beratan, J. Phys. Chem. 100 (1996) 17678.
[9] E.K. Wilson, C&EN, 11 March 1997.
[10] M.R. Arkin, E.D.A. Stemp, S.C. Pulver, J.K. Barton, Chem. Biol. 4 (1997) 389.
[11] H.M. McConnell, J. Chem. Phys. 35 (1961) 508.
[12] S. Larson, J. Am. Chem. Soc. 103 (1981) 4034.
[13] S. Priyadarshy, S.M. Risser, D.N. Beratan, J. Phys. Chem. 100 (1996) 17678.
[14] A.K. Felts, W.T. Pollard, R.A. Friesner, J. Phys. Chem. 99 (1995) 2929.
[15] T.L. Kunii, H. Kuroda, Theoret. Chim. Acta 11 (1968) 97.
[16] C. Desfrançois, H. Abdoul-Carime, J.P. Schermann, J. Chem. Phys. 104 (1996) 7792.
[17] J.H. Hendricks, S.A. Lyapustina, H.L. de Clercq, J.T. Snodgrass, K.H. Bowen, J. Chem. Phys. 104 (1996) 7788.

[18] C. Desfrançois, V. Periquet, Y. Bouteiller, J.P. Schermann, J. Phys. Chem. A 102 (1998) 1274.
[19] J.H. Hendricks, S.A. Lyapustina, H.L. de Clercq, K.H. Bowen, J. Chem. Phys. 108 (1998) 8.
[20] J. Smets, D.M.A. Smith, Y. Elkadi, L. Adamowicz, J. Phys. Chem. A 101 (1997) 9152.
[21] J. Smets, W.J. McCarthy, L. Adamowicz, J. Phys. Chem. 100 (1996) 14655.
[22] J.H. Hendricks, H.L. de Clercq, S.A. Lyapustina, C.A. Francher, T.P. Lippa, J.M. Collins, S.T. Arnold, G.H. Lee, K.H. Bowen, Structures and Dynamics of Clusters, Yamada Conference XLIII Proc., Universal Academy Press, Tokyo, 1996, and references therein.
[23] Ch. Desfrancois, H. Abdoul-Carime, J.-P. Schermann, Int. J. Mod. Phys. B 12 (1996) 1339, and references therein.
[24] J.A. Stockdale, F.J. Davis, R.N. Compton, C.E. Klots, J. Chem. Phys. 60 (1974) 4279.
[25] R.L. Jackson, A.H. Zimmerman, J.I. Brauman, J. Chem. Phys. 71 (1979) 2088.
[26] H. Haberland, C. Ludewigt, H.G. Schindler, D.R. Worsnop, J. Chem. Phys. 81 (1984) 3742.
[27] K.R. Lykke, R.D. Mead, W.C. Lineberger, Phys. Rev. Lett. 52 (1984) 2221.
[28] R.D. Mead, K.R. Lykke, W.C. Lineberger, J. Marks, J.I. Brauman, J. Chem. Phys. 81 (1984) 4883.
[29] O.H. Crawford, Mol. Phys. 20 (1971) 585.
[30] C. Desfrancois, H. Abdoul-Carime, N. Khelifa, J.P. Schermann, Phys. Rev. Lett. 73 (1994) 2436.
[31] C. Desfrancois, H. Abdoul-Carim, C. Adjouri, N. Kelifa, J.P. Schermann, Europhys. Lett. 26 (1994) 25.
[32] J. Schiedt, R. Weinkauf, manuscript submitted.
[33] N.A. Oyler, L. Adamowicz, J. Phys. Chem. 97 (1993) 11122.
[34] N.A. Oyler, L. Adamowicz, Chem. Phys. Lett. 219 (1994) 223.
[35] P. Hobza, Tschechische Akademie der Wissenschaften, Prag, 1997, personal communication.
[36] S.-P. Jiang, G. Raghunathan, K.-L. Ting, J.C. Xuan, R.L. Jernigan, J. Biomol. Struct. Dyn. 12 (1994) 367.
[37] D.A. Estrin, L. Paglieri, G. Corongiu, J. Phys. Chem. 98 (1994) 5653.
[38] J. Leszczyński, J. Phys. Chem. 96 (1992) 1649.
[39] R.B. Brown, P.D. Godfrey, D. McNaughton, A.P. Pierlot, J. Am. Chem. Soc. 110 (1988) 2329.
[40] I. Kulakowska, M. Geller, B. Lesyng, K. Bolewska, K.L. Wierzchowski, Biochim. Biophys. Acta 407 (1975) 420.
[41] J.S. Kwiatkowski, J. Leszczyński, J. Phys. Chem. 100 (1996) 941.
[42] H.-P. Weber, B.M. Craven, Acta Crystallogr. B 46 (1990) 532.
[43] M. Szczesniak, K. Szczepaniak, J.S. Kwiatkowski, K. KuBalat, W.B. Person, J. Am. Chem. Soc. 110 (1988) 8319.
[44] J. Cooper, R.N. Zare, J. Chem. Phys. 48 (1968) 942.
[45] G.H. Roehrig, N.A. Oyler, L. Adamowicz, J. Phys. Chem. 99 (1995) 14285.
[46] H. Abdoul-Carime, Y. Bouteiller, C. Desfrançois, L. Philippe, J.P. Schermann, Acta Chem. Scand. 51 (1997) 145.
[47] M. Gutowski, P. Skurski, J. Phys. Chem. B 101 (1997) 9143.
[48] M. Gutowski, K.D. Jordan, P. Skurski, J. Phys. Chem. A 102 (1998) 2624.
[49] D.M.A. Smith, J. Smets, Y. Elkadi, L. Adamowicz, Chem. Phys. Lett. 288 (1998) 609.
[50] S.Y. Han, J.H. Kim, J.K. Song, S.K. Kim, manuscript submitted.
[51] G. Markovich, S. Pollack, R. Giniger, O. Cheshnovsky, J. Chem. Phys. 101 (1994) 9344.
[52] D.W. Arnold, S.E. Bradforth, E.H. Kim, D.M. Neumark, J. Chem. Phys. 102 (1995) 3510.
[53] I.-C. Yeh, L. Perera, M.L. Berkowitz, Chem. Phys. Lett. 264 (1997) 31.
[54] J. Schiedt, R. Weinkauf, Chem. Phys. Lett. 266 (1997) 201.
[55] R. Weinkauf, J. Schiedt, F. Lehrer, E.W. Schlag, S. Rentsch, manuscript submitted.
[56] M.D. Sevilla, B.B. Besler, A.O. Colson, J. Chem. Phys. 98 (1994) 2215.
[57] W.J. Knott, J. Schiedt, R. Weinkauf, unpublished results.
[58] J. Schiedt, R. Weinkauf, Chem. Phys. Lett. 274 (1997) 18.
[59] K. Aflatooni, G.A. Gallup, P.D. Burrow, J. Phys. Chem. 102 (1998) 6205.
[60] M.D. Sevilla, B. Besler, A.-O. Colson, J. Phys. Chem. 99 (1995) 1060.
[61] D. Serxner, C.E.H. Dessent, M.A. Johnson, J. Chem. Phys. 105 (1996) 7231.
[62] J.E. Combariza, N.R. Kestner, J. Jortner, J. Chem. Phys. 100 (1994) 2851.
[63] J. Smets, W.J. McCarthy, L. Adamowicz, Chem. Phys. Lett. 256 (1996) 360.
[64] K.R. Lykke, K.K. Murray, D.M. Neumark, W.C. Lineberger, Phil. Trans. R. Soc. Lond. A 324 (1988) 179.
[65] L.A. Posey, M.J. Deluca, M.A. Johnson, Chem. Phys. Lett. 131 (1986) 170.
[66] J. Schiedt, R. Weinkauf, unpublished results.
[67] L. Lehr, M.T. Zanni, B.J. Greenblatt, R. Weinkauf, D.M. Neumark, manuscript submitted.
[68] W.G. Scherzer, H.L. Selzle, E.W. Schlag, R.D. Levine, Phys. Rev. Lett. 72 (1994) 1435.
[69] W.R. Garret, J. Chem. Phys. 73 (1980) 5721.
[70] K.P. Huber, Ch. Jungen, J. Chem. Phys. 92 (1990) 850.